

Band gap of wurtzite GaAs: A resonant Raman studyPatryk Kusch,^{1,*} Steffen Breuer,² Manfred Ramsteiner,² Lutz Geelhaar,² Henning Riechert,² and Stephanie Reich¹¹*Institut für Experimental Physik, Freie Universität, D-14195 Berlin, Germany*²*Paul Drude Institut für Festkörperelektronik, D-10117 Berlin, Germany*

(Received 5 June 2012; revised manuscript received 6 July 2012; published 24 August 2012)

We report resonant Raman scattering (RRS) by the TO, LO, and 2 LO modes of single wurtzite and zinc-blende GaAs nanowires. The optical band gap of wurtzite GaAs is $1.460 \text{ eV} \pm 3 \text{ meV}$ at room temperature, and $35 \pm 3 \text{ meV}$ larger than the GaAs zinc-blende band gap. Raman measurements using incoming light polarized parallel and perpendicular to the wire c axis allowed us to investigate the splitting of heavy Γ_9 and light-hole Γ_7 band at the Γ point of $65 \pm 6 \text{ meV}$.

DOI: [10.1103/PhysRevB.86.075317](https://doi.org/10.1103/PhysRevB.86.075317)

PACS number(s): 63.22.Gh, 78.30.Fs, 63.20.kd

I. INTRODUCTION

Nanowires (NWs) are quasi-one-dimensional crystals with well-defined diameters and a large aspect ratio. They have a huge potential for application in the field of optoelectronics (e.g., as light emitting diodes, photodetectors, and other applications¹⁻³). III-V semiconducting nanowires often crystallize in the wurtzite (WZ) structure, which is metastable in bulk material.^{4,5} Bulk GaAs has a zinc-blende (ZB) structure. Because of the lower surface energy of the WZ phase and the large surface-to-volume ratio of nanostructures, GaAs NWs can show a pure WZ, a pure ZB, or a mixture of the ZB and WZ phases.⁵

The properties, in particular, the band structure and fundamental gap E_0^{WZ} of WZ GaAs are controversially debated. The knowledge of the optical gap and the band structure of WZ NWs allows one to progress new NW-based devices in the field of optics, electronics, and biological sensing.⁶ The band gap E_0^{ZB} of ZB GaAs is 1.425 eV at room temperature and 1.519 eV at 0 K . Summarizing the currently published findings, a large fraction of currently available studies placed the WZ gap up to 20 meV below the gap of ZB GaAs,⁷⁻¹⁰ while another fraction reported the wurtzite gap up to 55 meV larger than the gap in the zinc-blende structure.¹¹⁻¹⁵ However, there is a broad consensus that the WZ-ZB interface in GaAs exhibits a type-II band alignment, where the conduction and valence band energy levels are higher in WZ than in ZB GaAs. Since the carrier diffusion length in GaAs is usually large (on the order of $1 \mu\text{m}$), electrons are very efficiently captured within ZB segments. This results in a large probability to predominantly observe luminescence at energies lower than the band-gap energies of either polytype, even if only a small number of ZB segments exists. Moreover, the presence of defect levels often favors the observation of luminescence at energies below that of the band gap, particularly, for measurements at low temperatures. Thus, a clear interpretation of low-temperature luminescence spectra of GaAs NWs with respect to the value of E_{WZ_0} is not straightforward. Jahn *et al.* performed CL investigations of GaAs NWs at room temperature, from which they suggested a lower bound of the difference $E_{\text{WZ}_0} - E_{\text{ZB}_0}$ of 55 meV . More reliable results regarding the band-gap energy can be derived from optical experiments which are directly related to the electronic density of states such as resonant Raman scattering.¹⁶ Choosing appropriate excitation energies and polarization conditions allow accessing various electronic

transitions, their symmetries, and selection rules. Ketterer *et al.* measured identical band-gap energies for the wurtzite and zinc-blende GaAs with resonant Raman scattering.¹⁷ They observed the energetically higher light-hole to conduction band transition. The study focused on the second-order LO resonances and omitted scattering by TO phonons. Peng *et al.*¹⁸ observed constant scattering intensities of the TO modes, a single LO resonance, and a shift of the Γ_{7C} conduction band to higher energies.

In this paper we perform resonant Raman experiments on ZB and WZ GaAs NWs with comparable diameters to determine the optical band gap E^{WZ} of WZ GaAs. Our measurements show consistently $E^{\text{WZ}} = 1.460 \text{ eV}$ at room temperature, 35 meV above the ZB gap, using TO, LO, and 2LO resonance profiles. By measuring Raman resonances with incoming light polarized parallel and perpendicular to the wire c axis we find a splitting of 65 meV between the heavy- and light-hole band at the Γ point of WZ GaAs. Our data allow a consistent assignment of the optically active transitions in WZ GaAs.

II. EXPERIMENTAL DETAILS

WZ GaAs nanowires with high phase purity were grown on Si(111) by molecular beam epitaxy (MBE) employing the Au-assisted vapor-liquid-solid (VLS) process. The detailed growth conditions were described in Ref. 19; the growth temperature was $500 \text{ }^\circ\text{C}$. These WZ nanowires grew along the [0001] direction and normal to the substrate. On average, their diameter was 50 nm and their length $2.2 \mu\text{m}$. WZ nanowires taken from the identical sample were already analyzed by photoluminescence, x-ray diffraction, and cathodoluminescence.²⁰

As a reference sample, ZB GaAs nanowires with high phase purity and 60-nm average diameters are used, which were grown using the self-assisted rather than the Au-assisted VLS process.²¹ Instead of oxide removal and Au deposition, the native oxide was left on the Si substrates to facilitate the formation of Ga droplets with appropriate size. For the ZB wires, the growth temperature was $580 \text{ }^\circ\text{C}$ and the As_4 flux was reduced by 25% in relation to that for the WZ nanowires. The remaining growth parameters were identical.

For the Raman experiments, NWs were removed from the growth substrate by ultrasonication in ethanol and dispersed on a Si substrate with markers for identification under

a light microscope. The solution was diluted to achieve single-nanowire measurements. For the resonant Raman experiments a Ti:Sa ring laser was used for excitation. The laser is fully tunable from 690 to 1050 nm. Raman spectra were recorded with a Horiba T64000 triple monochromator in backscattering configuration with a microscope and a motorized XY stage. After selecting one NW the resonant micro-Raman spectroscopy with a $100\times$ objective was performed at room temperature for wavelengths from 730 to 890 nm (1.39–1.69 eV). The light was chosen to be polarized along the nanowire axis [$x(z, z)\bar{x}$ configuration, where z is the growth axis c] and perpendicular to the axis [$x(y, y)\bar{x}$ configuration]. At each measurement the NW was excited at the same spot and with the same laser power of 3.5 mW. The intensity of the Raman spectra was calibrated using a CaF_2 crystal with a known and constant Raman cross section.¹⁶ The Raman peaks were fitted by Lorentzians and the intensities were determined by peak area integration.

III. RESULTS AND DISCUSSION

In Fig. 1(a) near resonant Raman spectrum of a single wurtzite GaAs NW is shown with the typical Raman modes for GaAs, a transversal optical (TO) phonon mode at 267 cm^{-1} and a longitudinal optical (LO) phonon mode at 293 cm^{-1} . The frequencies of the phonons are at the bulk position so we exclude strain and confinement effects. We also identify higher-order LO phonon modes in Fig. 1, which indicates that the Raman scattering for the LO phonon involves excitonic states.¹⁶ Finally, we observe photoluminescence around 855 nm (1.45 eV). This already points towards the WZ optical gap being larger than the ZB band gap. To investigate the exact resonance energy, we recorded Raman spectra as a function of excitation energy around 855 nm. In the following, we concentrate on the LO, TO, and second-order LO resonance.

In the literature two models for the band structure of WZ GaAs nanowires are discussed. The first model shows a

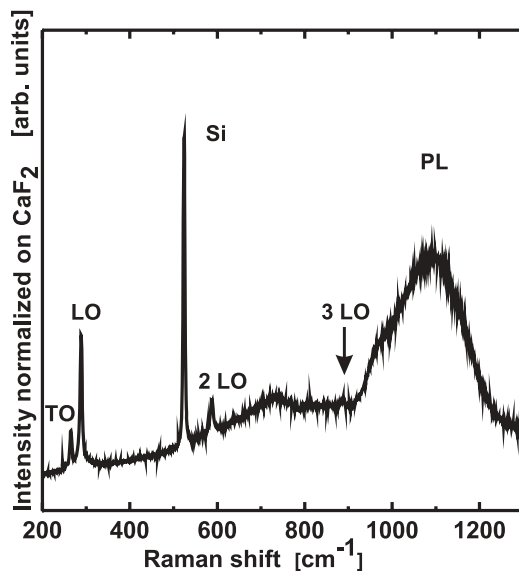


FIG. 1. Raman spectra of a single WZ GaAs NW with 50-nm diameter and $2.2\text{-}\mu\text{m}$ length at room temperature at 1.56-eV excitation.

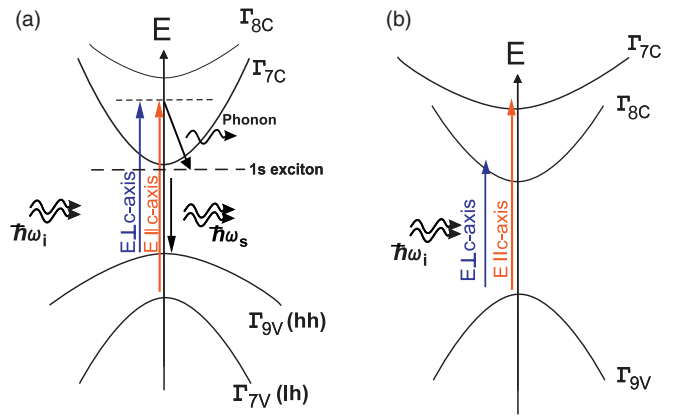


FIG. 2. (Color online) Alternative schematic band structure at the Γ point of wurtzite GaAs. (a) The valence bands are formed by the Γ_{9V} heavy-hole and the Γ_{7V} light-hole states. One of the conduction bands has Γ_{7C} symmetry. The energetic position of the Γ_{8C} conduction band is above the Γ_{7C} conduction band. Optical transitions are allowed for $\Gamma_{9V} \rightarrow \Gamma_{7C}$ under perpendicular and $\Gamma_{7V} \rightarrow \Gamma_{7C}$ under both parallel and perpendicular polarization of the incoming light. (b) The valence band is formed by the Γ_{9V} state; the lowest conduction band has Γ_{8C} symmetry.

splitting of the heavy-hole hh (Γ_{9V}) and light-hole lh (Γ_{7V}) band, as in Fig. 2(a).¹⁷ Alternatively discussed are a Γ_{9V} valence band and two conduction bands with Γ_{8C} and Γ_{7C} symmetry¹⁸ [see Fig. 2(b)]. The transition in Fig. 2(a) between the Γ_{7V} valence band (red arrow) and the Γ_{7C} conduction band is allowed for light polarized along and perpendicular to the wire c axis, the transition between Γ_{9V} valence band and the Γ_{7C} conduction band [blue arrow in Figs. 2(a) and 2(b)] is allowed only for light polarized perpendicular to the wire c axis.²² Transition between Γ_{9V} valence band and Γ_{8C} conduction band are allowed only for light polarized perpendicular to the wire axis.²² The two models differ strongly in the resulting optical selection rules.

In a resonant Raman process the enhancement from the ingoing resonance results when the energy of the incident light matches an allowed optical transition. For outgoing resonance an incoming photon $\hbar\omega_i$ excites an electron to a virtual state [Fig. 2(a)]. The state relaxes by inelastic scattering with the lattice. The recombination occurs again between real states and leads then to a Raman scattered photon $\hbar\omega_s$ with a strongly enhanced signal (see Fig. 2).¹⁶ Polarized Raman experiments will allow one to distinguish between the band structures and to determine the energetic positions of the bands.

In Fig. 3 we present the resonant Raman intensities of the TO phonon in WZ (circles) and ZB (triangles) GaAs NWs. The TO phonon showed a single, ingoing resonance in ZB GaAs at the gap $E_0^{\text{zb}} = 1.425\text{ eV}$, due to deformation potential, in excellent agreement with published data.²³ Clearly, the resonance in WZ GaAs is shifted by 35 meV to higher energies (see Fig. 3). This places $E^{\text{wz}} = 1.462\text{ eV}$ (i.e., higher than in ZB wires). The LO resonance profile for the WZ nanowire (black) and for a ZB reference sample (blue) are displayed in Fig. 4(a). In contrast to the single resonance of the TO mode, the LO profiles show an ingoing and outgoing resonance with a separation of one LO phonon energy (36 meV, Ref. 23). Compared to ZB GaAs, the resonances of the WZ GaAs are

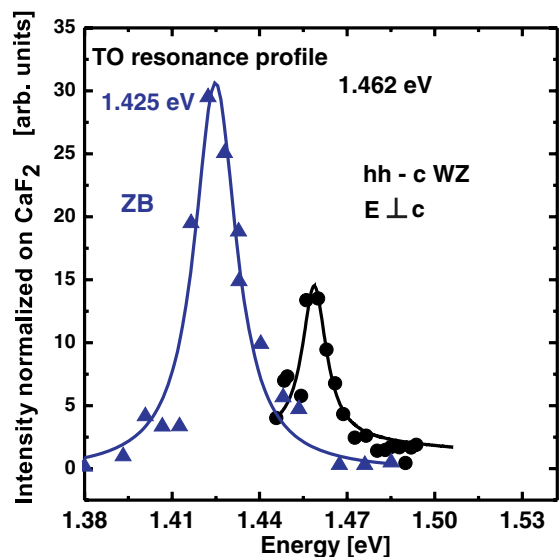


FIG. 3. (Color online) Resonant Raman profile of the TO mode from a single wurtzite GaAs nanowire for incident light polarized perpendicular to the NW c axis (black circles and solid line). For comparison the TO resonance profile (blue triangles and solid line) for zinc-blende GaAs NW is shown with light polarized along the wire axis. Both profiles were measured at room temperature.

again blue-shifted by 37 meV. At the ZB GaAs band gap neither for incident light parallel nor perpendicular to the NW c axis a resonance maximum occur in the WZ wire. Fröhlich coupling gives rise to strong multiphonon bands for excitonic resonances (see Fig. 1²³). Figure 4(b) shows the resonance profile of the second-order LO mode. The separation between ingoing and outgoing resonance is 72 meV, or twice to LO energy, as can be seen in Fig. 4(b). The ingoing resonance is at 1.459 eV (i.e., the same energy as the LO and close to the TO resonance).

The observation of an ingoing and outgoing LO resonance and the TO resonance profile allow us to determine the exact optical gap of WZ GaAs. From the ingoing LO and two LO resonance we estimate an optical band-gap energy of 1.459 eV. The outgoing resonances yield an optical band gap $E^{WZ} = 1.458$ eV. The TO resonance is 1.462 eV directly at the optical band-gap energy, as for ZB GaAs.²³ Combining all these Raman experiments show clearly that the optical WZ band gap is $1.460\text{eV} \pm 3$ meV at room temperature. Moreover the resonances in the range from 1.38 to 1.54 eV are strongly polarized perpendicular to the wire axis. They belong to $\Gamma_{9V} \rightarrow \Gamma_{7C}$ or $\Gamma_{9V} \rightarrow \Gamma_{8C}$ transition (see Fig. 2). Transitions between Γ_{9V} and Γ_{8C} bands are expected to be very weak.¹⁷ The strong 2LO resonance at 1.46 eV is a clear sign of the $\Gamma_{9V} \rightarrow \Gamma_{7C}$ transition.

We also performed Raman experiments with light polarized parallel to the NW c axis in the energy range between 1.53 and 1.60 eV [$x(z,z)\bar{x}$ configuration]. The resonance profiles of the TO and the one and two LO phonon modes in parallel configuration for the wurtzite NW are displayed in Fig. 5. The TO profile shows an ingoing resonance, which is typical for RRS by deformation potential.²³ The LO and 2LO profiles show outgoing resonances, as expected for RRS by Fröhlich coupling.¹⁶

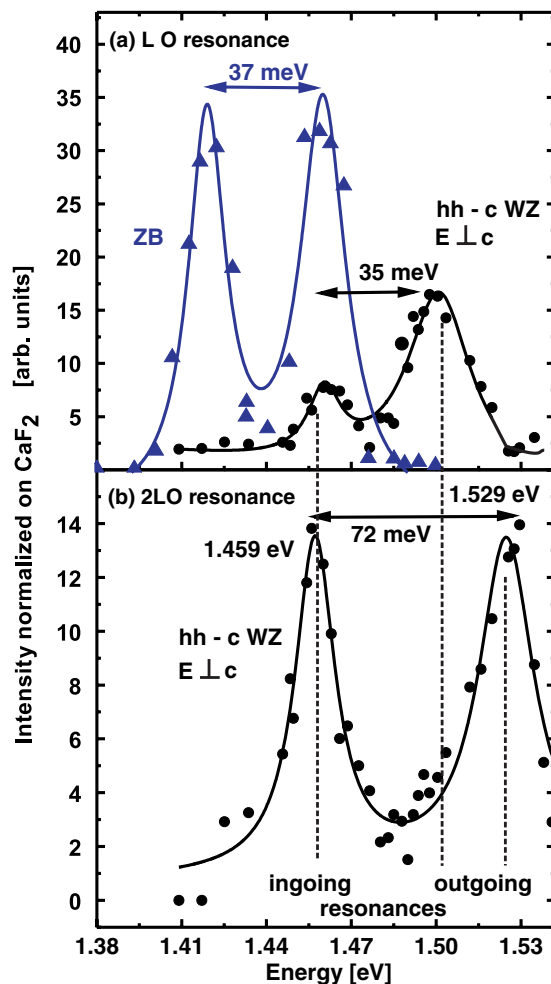


FIG. 4. (Color online) (a) Resonant Raman profiles of the LO mode (incident light polarized perpendicular to NW c axis) from a single WZ GaAs NW (black circles and solid line) and ZB GaAs reference sample (blue triangles and solid line). (b) 2 LO resonance profile for incident light polarized perpendicular to the NW c axis. All profiles were collected at room temperature.

The resonances are strongly polarized parallel to the wire axis, which means that the resonant enhancement of the intensity is now due to the resonant Raman process between Γ_{7C} conduction and Γ_{7V} valance (light-hole) band (Fig. 2, red arrow).²² From the maxima at 1.561 eV for the LO phonon, 1.596 eV for the two LO phonon, and 1.527 eV for the TO we determine a transition energy $E(\Gamma_{7V} \rightarrow \Gamma_{7C}) = 1.528\text{eV} \pm 3$ meV. This yields to a splitting between the heavy and light hole of 65 ± 6 meV, much lower then the 103 meV observed by Ketterer *et al.*¹⁷ Note, however, that the discrepancy is due to the smaller fundamental gap reported in Ref. 17. From the determined values for $E(\Gamma_9 \rightarrow \Gamma_7)$ and $E(\Gamma_7 \rightarrow \Gamma_7)$ we calculate the crystal field splitting Δ_1 ,²⁴

$$E(\Gamma_{9v}) = E_0 + \Delta_1 + \Delta_2, \quad (1)$$

and

$$E(\Gamma_{7v}) = E_0 + \frac{\Delta_1 + \Delta_2}{2} \pm \frac{\sqrt{(\Delta_1 - \Delta_2)^2 + 8\Delta_3^2}}{2}, \quad (2)$$

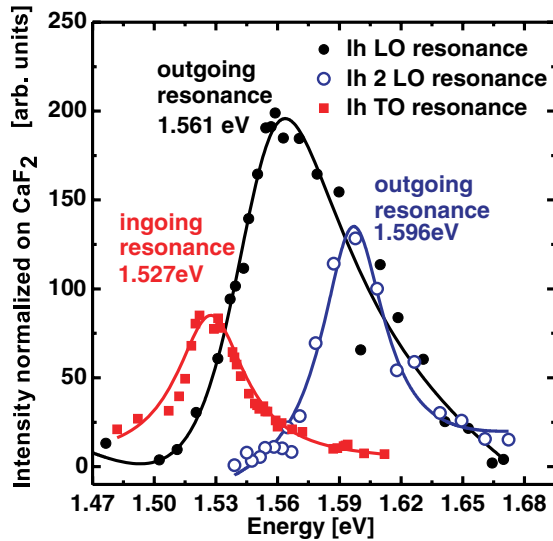


FIG. 5. (Color online) lh-c resonance profile from a single WZ GaAs NW at room temperature for light polarized parallel to the nanowire axis. TO intensity, squares; LO intensity, solid circles; 2LO intensity, open circles.

with an average value for the two matrix elements Δ_2 and Δ_3 (required to describe the spin-orbit interaction) of typically 350 meV for wurtzite GaAs. The crystal field splitting energy then amounts to $\Delta_1 \sim 110$ meV. Our calculated value is in excellent agreement with the theoretical prediction $\Delta_1 = 122$ meV by Murayama *et al.*¹⁴

Our result for the band-gap energy of wurtzite GaAs assumes an exciton binding energy (4 meV) as found in zincblende GaAs. The differences in exciton binding between the two crystal structures are expected to be small. Nevertheless, a better knowledge of the excitonic properties of wurtzite GaAs is highly desirable to remove the systematic uncertainty in the reported band-gap energies. Note that the heavy-light hole splitting is hardly affected by this uncertainty.

We now compare our resonance profiles and their interpretation to previous work. Peng *et al.* observed a single resonance

of the LO phonon at 1.56 eV at room temperature and under polarization parallel to the wire axis.¹⁸ It corresponds to our resonance profile in Fig. 5 with the comparable resonance 1.561 eV for the first-order LO. Ketterer *et al.*¹⁷ found a similar resonance at 1.66 eV; the shift to higher energies is due to the low-temperature (10-K) measurements in Ref. 17. This resonance was assigned to the $\Gamma_{7V} \rightarrow \Gamma_{7C}$ transition [compare Fig. 2(a)] in all three studies. We further confirm the $E(\Gamma_{7V} \rightarrow \Gamma_{7C}) = 1.561$ eV transition energy from the 2LO and the TO profile (see Fig. 5). Under perpendicular polarization we observe an ingoing and outgoing resonance of the first- and second-order LO phonon corresponding to the $\Gamma_{9V} \rightarrow \Gamma_{7C}$ transition at 1.462 eV. In contrast, Ketterer *et al.*¹⁷ found the LO profiles in resonance with ZB transition energies. Unfortunately, they do not show data in the 1.62–1.67 eV energy range where we expect the outgoing WZ $E(\Gamma_{9V} \rightarrow \Gamma_{7C})$ resonance at low temperatures. The origin of the discrepancy remains unclear. A larger optical gap for WZ GaAs at room temperature is in excellent agreement with recent luminescence data^{11–14}; importantly, cathodoluminescence on similar nanowires found also a larger WZ bandgap.²⁰

IV. CONCLUSION

We investigated single wurtzite GaAs nanowires by resonant Raman scattering. The resonance of the TO, LO, and 2LO modes yield consistently transition energies $E(\Gamma_{9V} \rightarrow \Gamma_{7C}) = 1.460 \text{ eV} \pm 3 \text{ meV}$ and $E(\Gamma_{7V} \rightarrow \Gamma_{7C}) = 1.528 \text{ eV} \pm 3 \text{ meV}$. The optical gap in WZ GaAs is $35 \pm 3 \text{ meV}$ larger than in ZB. The heavy-light hole splitting amounts to $65 \pm 3 \text{ meV}$. For the exact position of the Γ_{8C} conduction band and thus the size and character of the fundamental gap in WZ GaAs, nonoptical experiments are highly desirable.

ACKNOWLEDGMENTS

We thank Christian Lehmann for helpful discussions and the European Research Council under Grant No. 210642 for financial support.

*patryk.kusch@fu-berlin.de

¹C. M. Lieber and Z. L. Wang, *MRS Bull.* **32**, 99 (2007).

²R. Agarwal and C. M. Lieber, *Appl. Phys. A: Mater. Sci. Process* **85**, 209 (2006).

³C. Thelander, P. Agarwal, S. Brongersma, J. Eymery, L. Feiner, A. Forchel, M. Scheffler, W. Riess, B. Ohlsson, U. Gösele *et al.*, *Materials Today* **9**, 28 (2006).

⁴M. I. McMahon and R. J. Nelmes, *Phys. Rev. Lett.* **95**, 215505 (2005).

⁵K. A. Dick, P. Caroff, J. Bolinsson, M. E. Messing, J. Johansson, K. Deppert, L. R. Wallenberg, and L. Samuelson, *Semicond. Sci. Technol.* **25**, 024009 (2010).

⁶P. Caroff, J. Bolinsson, and J. Johansson, *IEEE J. Sel. Top. Quant. Electron* **17**, 829 (2011).

⁷M. Heiss, S. Conesa-Boj, J. Ren, H.-H. Tseng, A. Gali, A. Rudolph, E. Uccelli, F. Peiró, J. Morante, D. Schuh *et al.*, *Phys. Rev. B* **83**, 045303 (2011).

⁸M. Moewe, L. C. Chuang, S. Crankshaw, C. Chase, and C. Chang-Hasnain, *Appl. Phys. Lett.* **93**, 023116 (2008).

⁹A. De and C. E. Pryor, *Phys. Rev. B* **81**, 155210 (2010).

¹⁰Z. Zanolli, F. Fuchs, J. Furthmüller, U. von Barth, and F. Bechstedt, *Phys. Rev. B* **75**, 245121 (2007).

¹¹D. Spirkoska, J. Arbiol, A. Gustafsson, S. Conesa-Boj, F. Glas, I. Zardo, M. Heigoldt, M. H. Gass, A. L. Bleloch, S. Estrade *et al.*, *Phys. Rev. B* **80**, 245325 (2009).

¹²T. B. Hoang, A. F. Moses, H. L. Zhou, D. L. Dheeraj, B. O. Fimland, and H. Weman, *Appl. Phys. Lett.* **94**, 133105 (2009).

¹³F. Martelli, M. Piccin, G. Bais, F. Jabeen, S. Ambrosini, S. Rubini, and A. Franciosi, *Nanotechnology*, **18**, 125603 (2007).

¹⁴M. Murayama and T. Nakayama, *Phys. Rev. B* **49**, 4710 (1994).

¹⁵R. Gurwitz, A. Tavor, L. Karpeles, I. Shalish, W. Yi, G. Seryogin, and V. Narayanamurti, *Appl. Phys. Lett.* **100**, 191602 (2012).

¹⁶M. Cardona and G. Güntherodt, *Light Scattering in Solids II* (Springer, Berlin/Heidelberg/New York, 1982).

- ¹⁷B. Ketterer, M. Heiss, E. Uccelli, J. Arbiol, and A. F. i Morral, *ACS Nano* **5**, 7585 (2011).
- ¹⁸W. Peng, F. Jabeen, B. Jusserand, J. C. Harmand, and M. Bernard, *Appl. Phys. Lett.* **100**, 073102 (2012).
- ¹⁹S. Breuer, M. Hilse, A. Trampert, L. Geelhaar, and H. Riechert, *Phys. Rev. B* **82**, 075406 (2010).
- ²⁰U. Jahn, J. Lähnemann, C. Pfüller, O. Brandt, S. Breuer, B. Jenichen, M. Ramsteiner, L. Geelhaar, and H. Riechert, *Phys. Rev. B* **85**, 045323 (2012).
- ²¹S. Breuer, C. Pfüller, T. Flissikowski, O. Brandt, H. T. Grahn, L. Geelhaar, and H. Riechert, *Nano Lett.* **11**, 1276 (2011).
- ²²P. Tronc, Y. E. Kitaev, G. Wang, M. F. Limonov, A. G. Panfilov, and G. Neu, *Phys. Status Solidi B* **216**, 599 (1999).
- ²³M. Brewster, O. Schimek, S. Reich, and S. Gradecak, *Phys. Rev. B* **80**, 201314 (2009).
- ²⁴B. Gil, O. Briot, and R.-L. Aulombard, *Phys. Rev. B* **52**, 17028 (1995).